MABS
2025, VOL. 17, NO. 1, 2483272
https://doi.org/10.1080/19420862.2025.2483272

Taylor & Francis
Taylor & Francis Group

REPORT

Rapid affinity-based purification of multi-specific antibodies using Kappa Select and Protein L

Kalie Mix*, Tingwan Sun*,#, Brian Hall, Jocelyn Newton##, Christina Eng, Yongjing Guo, and David Reczek

Sanofi US Large Molecule Research, Cambridge, MA, USA

ABSTRACT

Multispecific antibodies (msAbs) are becoming more prevalent as formats of choice for therapeutic antibody development due to their ability to modulate multiple biological targets. However, msAbs present unique protein production challenges due to product-related impurities, which are difficult to remove without loss of the protein of interest. Here, we report a versatile approach to remove product-related impurities by altering the binding affinity of light chains to Kappa Select (KS) or Protein L (Pro-L) resins. Introduction of amino acid mutations in the constant light chain domain or Framework 1 of the light chain abolished binding to KS and Pro-L resins, respectively, while antigen binding affinity remained intact. These purification-enabling mutations (PEMs) did not affect the thermal stability or purity of the proteins tested. In conjunction with PEMs, we demonstrate the design and application of an entirely affinity-based purification scheme employing Protein A (Pro-A), followed by KS and Pro-L affinity resins, to remove light chain mispaired species in Y-shaped bispecific antibodies and crossover dual variable domain (CODV) tri-specific antibodies. In principle, this purification scheme could be applied to any IgG-like msAb since it is compatible with Fc knobs-into-holes mutations and Fab arm charge-pair mutations. Moreover, it should be adaptable across a range of production scales and medium to high-throughput purification workflows within early-stage research.

ARTICLE HISTORY
Received 14 January 2025
Revised 17 March 2025
Accepted 18 March 2025

KEYWORDS
Bispecific antibodies; CODV; multi-specific antibodies; protein purification; trispecific antibodies

Introduction

Monoclonal antibodies have proven to be effective therapeutics for a variety of indications, with nearly 200 antibody therapies approved globally[1] and record numbers undergoing regulatory review.[2] Despite this success, a substantial number of indications remain for which only a minority of patients achieve a satisfactory clinical response to monospecific antibody therapy.[3] As a result, there is growing interest in the therapeutic potential of multi-specific antibodies (msAbs).[4] In addition to their ability to modulate multiple biological targets, msAbs confer the advantage of enabling novel functionalities that are not possible using a mixture of the monospecific parental antibodies.[5] Among the msAbs in the clinical pipeline, a common mechanism of action is bridging of cells by in-*trans* binding to redirect cytotoxic activity of effector cells,[6] but other mechanisms, such as receptor activation or inhibition, also hold great potential.

Numerous msAb formats that vary in size, valency, symmetry, and similarity to natural IgGs have been developed.[5] Selection of the optimal format hinges on factors specific to each disease indication, such as the desired geometry of the molecule relative to its binding targets, ability to elicit Fc effector function, and pharmacokinetic/pharmacodynamic properties. One msAb format known as cross-over dual variable Ig-like protein (CODV) overcomes many of the major limitations of other formats by using a circular self-contained architecture to promote a defined paratope orientation, which minimizes positional effects on antigen binding affinity.[7] This format bears close similarity to a natural IgG, with an Fc domain that can enable effector function and long serum half-life. CODVs can be designed to contain either two or three antigen-binding domains (bsCODV and tsCODV, respectively).

A challenge faced by the tsCODVs, as well as many other asymmetric msAb formats, is the proper assembly of light and heavy chains. The four distinct polypeptide chains which comprise the tsCODVs (two heavy and two light chains) can form multiple mispaired molecules; the most common are shown in Figure 1. Mutation of amino acids in the CH3 domain ("knobs-into-holes") is widely used to favor heterodimerization of the heavy chains,[8] but light chain mispairing remains a significant challenge. The presence of mispaired molecules creates difficulty in the production of tsCODVs and hinders downstream functional assays, thus convoluting the data needed for early selection of lead molecules. Much progress has been made in minimizing the amount of product-related impurities by introducing mutations, especially at the CH1:CL interface or eliminating ProA binding of the hole:hole homodimer ("RF" mutation),[9] but such mutations are not a 'one size fits all' solution and often do not fully resolve

CONTACT David Reczek David.Reczek@sanofi.com Sanofi US Large Molecule Research, 350 Water St, Cambridge, MA 02141, USA
*These authors contributed equally.
#Present address: Cambridge Antibody Labs, LLC, Framingham, MA, USA
##Present address: Sanofi Vaccines, Cambridge, MA, USA
Supplemental data for this article can be accessed online at https://doi.org/10.1080/19420862.2025.2483272

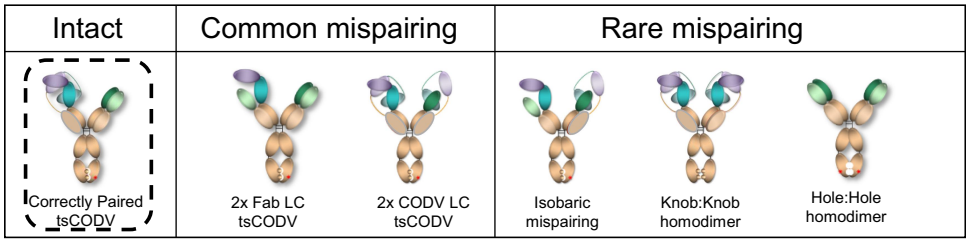

Figure 1. Intact and chain-mispaired trispecific CODV antibodies (tsCODV).

mispairing.[10–13] The chain pairing issue can also be addressed by alternative formats beyond a Y-shaped asymmetrical bsAb, for example, the "bipod" bsAbs described by Nesspor *et al.* These molecules contain an Fc bearing a Fab on one HC and an scFv on the other, which is amenable to high-throughput purification via CH1 chromatography.[14] Here, as an adjunct to such protein engineering approaches, we focus on the development of a rapid, all affinity-based purification strategy to remove light chain-mispaired molecules.

A typical tsCODV purification approach consists of a Pro-A capture step followed by ion-exchange (IEX) or hydrophobic interaction chromatography (HIC) and finished with size-exclusion chromatography (SEC). This approach has several drawbacks, as the imperfect resolution of IEX, HIC, and SEC columns often results in mixed fractions and subsequent loss of the protein of interest (POI). Additionally, this purification scheme often requires pilot-testing on a small scale before producing novel molecules at the desired scale, which prohibits its incorporation into high-throughput purification platforms. In contrast, an ideal purification strategy for discovery research would have the following characteristics: 1) employs entirely affinity-based chromatography methods to minimize loss of POI in mixed fractions, 2) universal or broad applicability to any IgG-based msAb, 3) ability to be incorporated in a high-throughput protein production platform, and 4) compatibility with other strategies, such as protein engineering or expression optimization, that favor proper chain assembly.

One potential approach to removing light chain-mispaired tsCODVs is to use commercially available light chain-binding chromatography resins, such as Protein L (Pro-L) and Kappa Select (KS). KS resin consists of an anti-kappa VHH that binds human kappa light chains primarily in the constant (Ck) and hinge (Vk – Ck) regions with high affinity.[15] Pro-L binds to the framework region of Vk1, Vk3, and Vk4 light chain subtypes, which are present in the majority of the human Ig repertoire.[16] Previous studies have reported a method for separating molecules based on Pro-L binding valency, for example, when one molecule contains two kappa light chains and another contains one each of kappa and lambda.[17] Our aim was to instead introduce a mutation in each tsCODV light chain that knocks out KS or Pro-L binding, which could enable the removal of mispaired molecules that lack one light chain or the other. We present here a purification strategy for the removal of mispaired multi-specific CODVs, which consists entirely of affinity-based chromatography steps and uses strategic mutations that knock out binding to light chain-binding ligands. This strategy results in high yield and purity of tsCODVs and can theoretically be applied to virtually any msAb format that contains two distinct light chains.

Results

Pro-L affinity purification efficiently removes a light-chain mispaired msAb with non-Pro-L-binding light chains

Pro-L is an Ig-binding protein originally isolated from *Peptostreptococcus magnus* that interacts with Framework 1 in the V-region of κ-LC from κ1, κ3 and κ4 subtypes, but not to κ2 and λ subtypes.[18] Before embarking on extensive engineering efforts, we first sought to determine whether Pro-L purification would remove a mispaired tsCODV, which naturally lacks Pro-L binding. The four distinct polypeptide chains (two heavy and two light) that comprise the tsCODVs can form multiple mis-paired molecules. The most common ones contain two copies of either the Fab light chain ("2× Fab LC tsAb") or CODV light chain ("2× CODV LC tsAb"), rather than one of each. We used Pro-L affinity purification to remove 2× Fab LC tsAb, which contains only Vκ2 light chains (Figure 2a).

The tsCODV was expressed using the Expi293 system and purified using a Pro-A affinity column as the first step. The eluted protein was further purified using a Pro-L column. Analysis of the flow through and eluate using sodium dodecyl sulfate polyacrylamide gel electrophoresis (SDS-PAGE) (Figure 2b) demonstrated that the Pro-L flowthrough contained only 2× Fab LC tsAb, suggesting that Pro-L purification can efficiently remove a mispaired species that lacks Pro-L binding.

Framework region 1 mutations in mAb light chain decrease or abolish Pro-L binding

To apply this method to molecules containing Pro-L binding light chains, such as κ1, κ3 and κ4 subtypes, we aimed to design mutations that universally abolish Pro-L binding for all kappa light chains. We used adalimumab, an anti-tumor necrosis factor (TNF) monoclonal antibody, as a test article. Eleven mutations to Framework 1 were designed using both sequence and structural information to make the adalimumab kappa light chain (Vκ1–27) resemble Vκ2 and λ light chains (Table 1). Wild-type adalimumab and 11 mutation-containing variants were expressed using the Expi293 system, and production titers were measured after Pro-A affinity purification. Characterization of Pro-L binding affinity of the proteins using biolayer

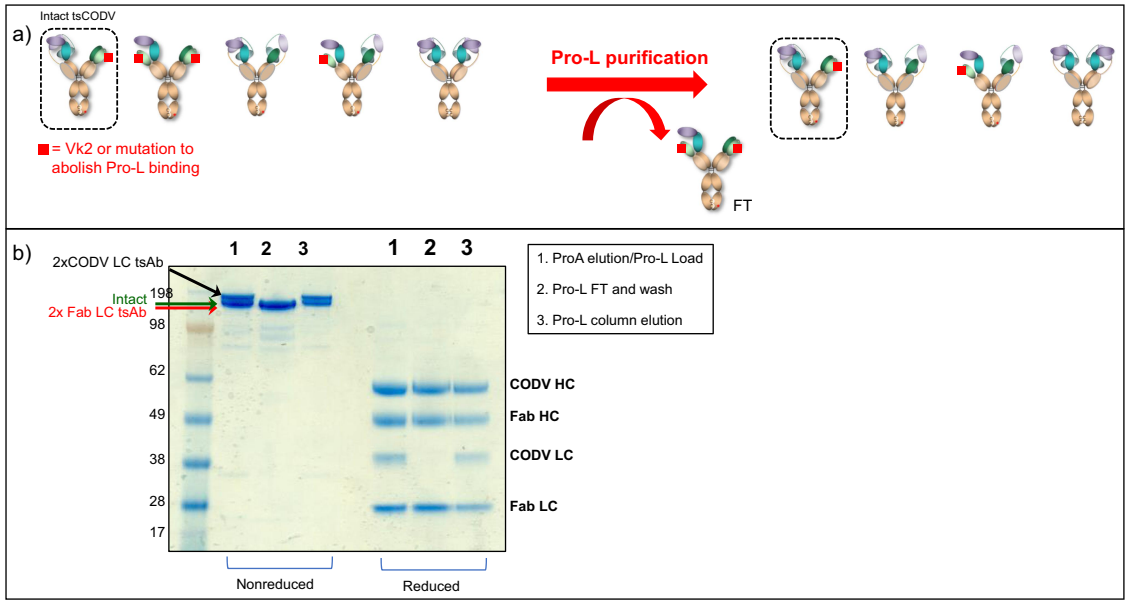

Figure 2. Pro-L concept test: Protein L purification of a trispecific antibody (tsCODV) with a non-pro-L binding arm. a. Removal of mispaired 2× Fab LC msAb in tsCODV by pro-L affinity purification following pro-A affinity purification. If the fab arm of a tsCODV consists of a non-pro-L-binding human IgG light chain (such as Vλ, or Vk2 subtype), the mispaired 2× Fab LC msAb is expected to flow through pro-L resin while the correctly paired tsCODV will bind to pro-L resin and be eluted from the column. b. SDS-PAGE comparison of pro-A eluate, pro-L flow-through, and pro-L neutralized eluate. In the flow through, only 2× Fab LC tsCODV mispaired species was detected; while in the pro-L elution, the correctly paired molecule together with 2× CODV LC tsCODV was detected.

Table 1. Sequences of 11 adalimumab mutants designed and tested for abolishing pro-L binding. Mutations were made in light chain framework region 1.

Mutant No.	Name																										
		1	2	3	4	5	6	7	8	9	10	11	12	13	14	15	16	17	18	19	20	21	22	23	24	25	26
	Wild Type	D	I	Q	M	T	Q	S	P	S	S	L	S	A	S	V	G	D	R	V	T	I	T	C	R	A	S
1	R18T/T20R																		T		R						
2	delS7							–																			
3	S9R/R18T/T20R									R									T		R						
4	S9R									R																	
5	S9P									P																	
6	R18T																		T								
7	delS7/S9P							–		P																	
8	S12P												P														
9	S12P/R18P												P						P								
10	R18P																		P								
11	S7P							P																			

interferometry (BLI) (Octet) showed that some mutations abolished binding to the Pro-L ligand (Figure 3a). These variants were further characterized by their ability to bind a Pro-L column. Among them, delS7/S9P and S12P showed decreased binding to the Pro-L column and appeared in the flowthrough or mild elution (pH 3.5) fractions, while wild-type adalimumab could only be eluted with more stringent elution (pH 2.5) (Figure 3b). Complete loss of Pro-L binding was observed in the BLI assay for the variant harboring the S12P/R18P mutation combination, which also flowed through the Pro-L column making this mutation set the top choice of those tested. The S12P/R18P mutant had similar analytical size-exclusion chromatography (aSEC) purity as wild-type adalimumab after a single step of Pro-A purification (Figure 4a) and did not show significant aggregation or fragmentation after stress treatment as assessed by aSEC and SDS-PAGE (Supplemental Figure S1). NanoDSF analysis demonstrated a small decrease in thermal stability relative to adalimumab (71.7°C for wild-type vs 68.0°C for S12P/R18P) (Figure 4b). All variants approximated wild-type levels of binding affinity for the target ligand, TNF (Figure 5).

Vκ–Cκ hinge mutations in mAb light chain knock out KS ligand binding

Next, we sought to develop a purification method to use in combination with Pro-L so that multiple light-chain-mispaired msAb species could be removed from a Pro-A eluate. In principle, an msAb containing two copies of light chains with Pro-L knockout mutations (described above) would first be removed by a Pro-L purification step, and an msAb containing two copies of light chains with KS knockout mutations would be removed in a subsequent step.

The crystal structure of an anti-kappa VHH domain binding to an antibody Ck domain shows that the VHH interacts with the Vκ–Cκ hinge through several key amino acids, such as T109, V110, and Q199.[15] Ereño-Orbea *et al.* also showed that when the

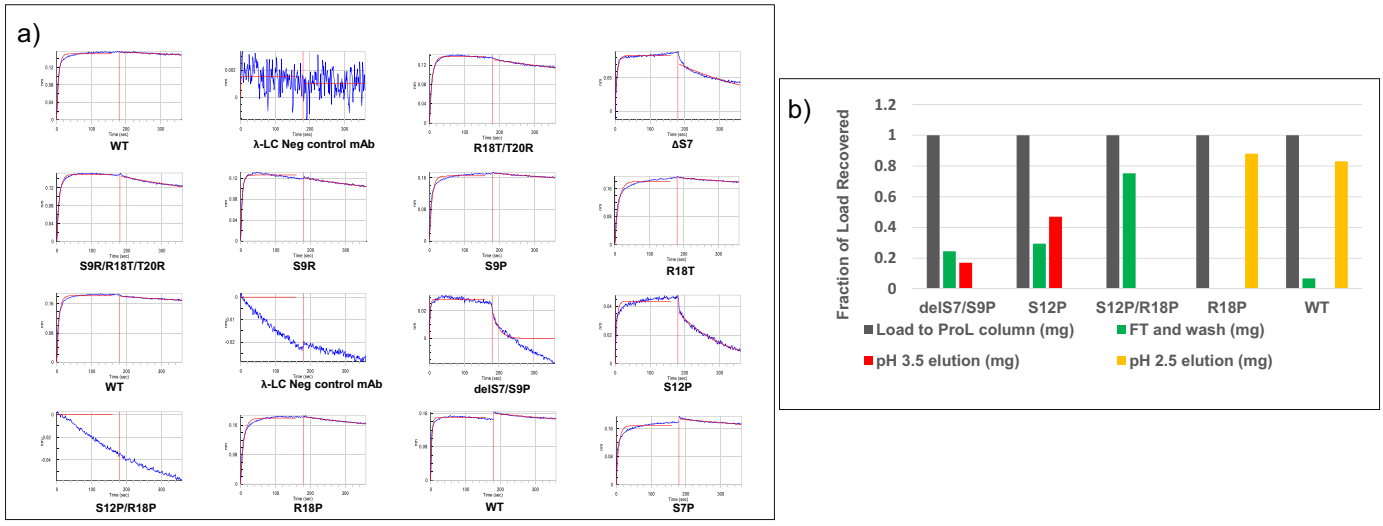

Figure 3. Characterization of wild-type adalimumab and pro-L knockout variants. a. Biolayer interferometry characterization of pro-L knockout mutants binding to pro-L ligand in solution. Binding was most significantly disrupted in the S12P/R18P double mutant. b. Analysis of protein recovered in pro-L load, flowthrough, and eluate fractions for WT adalimumab and pro-L KO mutants. Similar to the BLI results presented in B, the S12P/R18P double mutant did not bind to the pro-L resin and was only observed in the flow through and wash fraction.

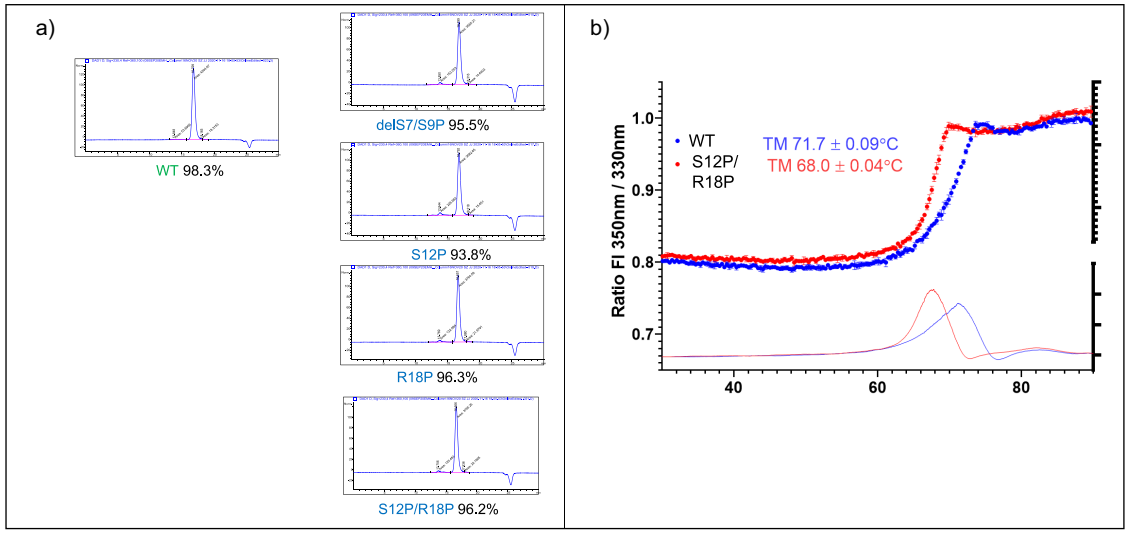

Figure 4. Biophysical characterization of adalimumab WT and Pro-L KO mutants. a. Analytical size exclusion chromatography (aSEC) chromatograms of adalimumab wild type and four pro-L KO mutants showed a high degree of purity for all samples tested with high similarity between WT and the S12P/R18P double mutant. b. NanoDSF characterization of wild-type adalimumab and pro-L KO variant S12P/R18P (T_m values) showed a slight reduction in thermal stability of the S12P/R18P double mutant.

human Vκ–Cκ hinge was replaced with the mouse sequence (A109, D110) in a human Fab, it no longer bound to an anti-kappa VHH ligand. Based on these data, we designed three mutants (Q199K, T109A/V110D, and T109A/V110D/Q199K) in the adalimumab kappa light chain and tested binding to the anti-kappa VHH ligand. Wild-type and the three variants of adalimumab were expressed using the Expi293 system and purified by a single step using Pro-A affinity chromatography. A BLI binding assay demonstrated that all three light chain variants lost binding to the KS ligand (Figure 6a), in contrast to the wild-type protein, which showed strong binding. In agreement with the BLI binding results, all three adalimumab light chain variants flowed through a KS column, while the wild-type adalimumab remained bound to the column (Figure 6b). The mutants had similar aSEC purity as wild-type adalimumab after a single step of Pro-A purification (Figure 7a) and did not show significant aggregation or fragmentation after stress treatment as assessed by aSEC and SDS-PAGE (Supplemental Figure S2). A nanoDSF assay demonstrated that these variants had similar thermal stability as the wild-type protein in the IgG format (Figure 7b), and a differential scanning calorimetry (DSC) assay demonstrated similar thermal stability at the F (ab)'2 level (Supplemental Figure S3). Another BLI assay was performed to check whether these mutations affected binding to the adalimumab target, TNF. All variants containing these mutations retained wild-type levels of antigen-binding affinity (Figure 8). Combined, these data suggest three potential candidate light chain mutations to knock out KS binding.

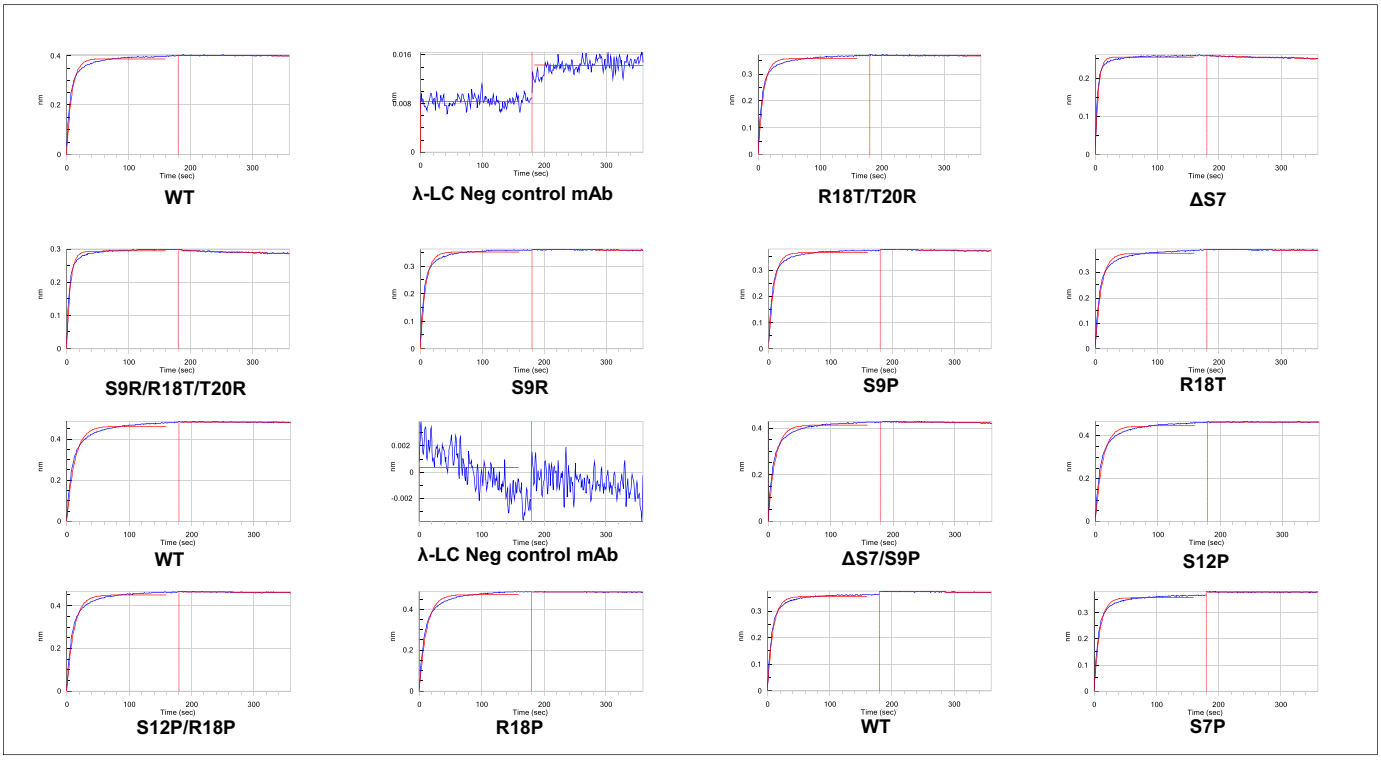

Figure 5. Biolayer interferometry characterization of wild-type adalimumab and pro-L knockout mutants binding to TNFα ligand in solution.

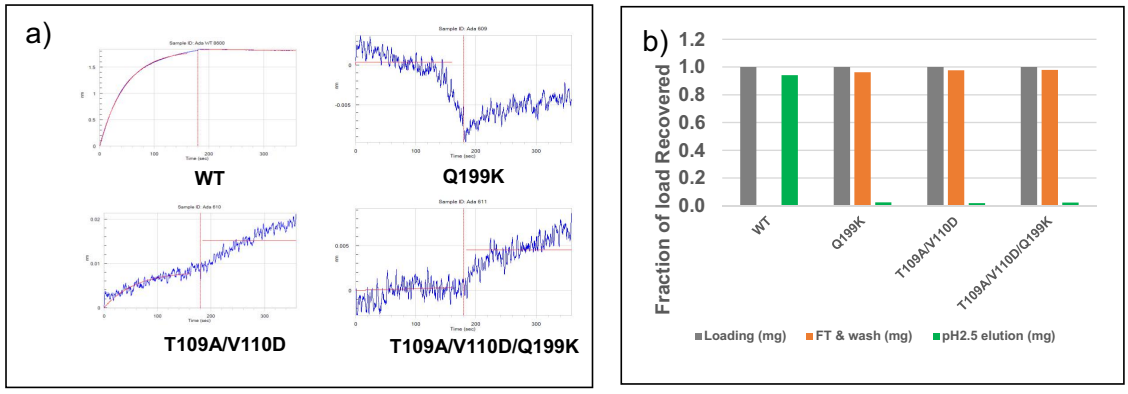

Figure 6. Characterization of wild-type adalimumab and KS knockout variants. a. Biolayer interferometry characterization of KS knockout mutants binding to KS ligand in solution demonstrated that all three mutations abolish binding to the KS ligand. b. Analysis of protein recovered in KS load, flowthrough, and eluate fractions for WT adalimumab and KS mutants.

KS affinity purification efficiently removes light-chain mispaired msAbs with KS knockout mutations

A tsCODV with a single Q199K mutation in its CODV light chain and RF mutation[9] in the CH2 domain was expressed using the Expi293 system and purified using Pro-A followed by KS chromatography. SDS-PAGE demonstrated the presence of 2× CODV LC tsAb, 2× Fab LC tsAb, and the desired intact tsAb in the Pro-A eluate (Figure 9). The KS flow through and two low pH elution fractions (pH 1.7 and 2.5) were collected and analyzed by SDS-PAGE. The KS flow through mainly contained the 2× CODV LC tsAb as expected, while the eluate did not have this mis-paired contaminant (Figure 9), indicating that the KS knockout mutation on the CODV arm enabled removal of the 2× CODV LC tsAb species.

Next, the KS binding knockout mutation Q199K was introduced solely on the Fab light chain of a CODV tsAb to test whether the mutation would enable removal of the 2× Fab LC tsAb. Proteins were expressed in the Expi293 system and purified by Pro-A followed by KS affinity chromatography. As shown by SDS-PAGE, the flow through contained the 2× Fab LC tsAb without a CODV light chain (Figure 10). These combined results indicate that the KS binding knockout mutation could be used either on the CODV light chain or the Fab light chain to remove the light chain mis-paired species.

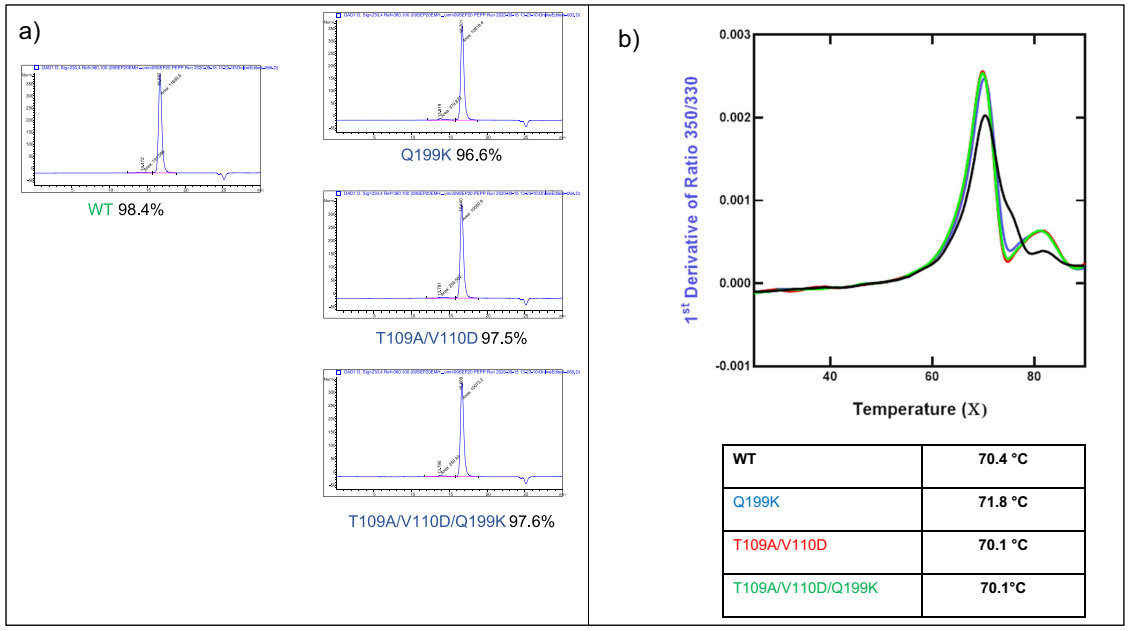

WT	70.4 °C
Q199K	71.8 °C
T109A/V110D	70.1 °C
T109A/V110D/Q199K	70.1°C

Figure 7. Biophysical characterization of adalimumab WT and KS knockout mutants. a. Analytical size exclusion chromatography (aSEC) chromatograms of adalimumab wild type and three KS knockout mutants. b. NanoDSF characterization of wild-type adalimumab and KS knockout mutant T_m values.

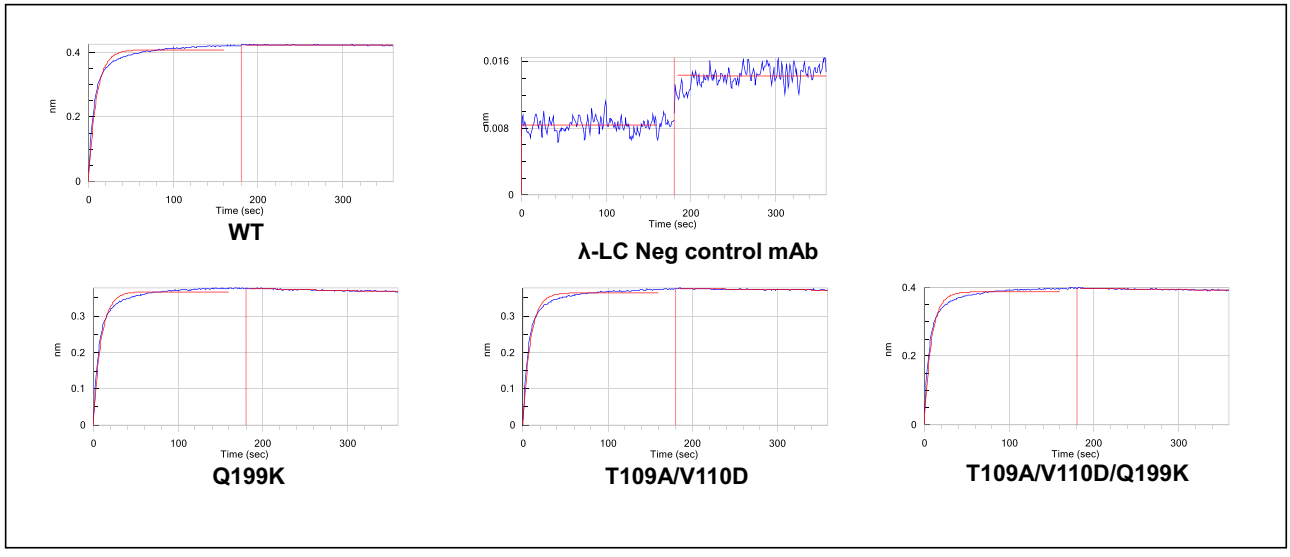

Figure 8. Biolayer interferometry characterization of wild-type adalimumab and KS knockout mutants binding to TNFα ligand in solution.

Removal of multiple mis-paired light chain species in tsCODVs using both Pro-L and KS affinity purification

We next tested the ability to combine the KS and Pro-L steps in sequence to remove both light chain mispaired species from the Pro-A eluate. In the first approach, we tested a tsCODV containing a Vκ2 light chain on the Fab arm that lacks Pro-L binding, a Q199K mutation on the CODV light chain which abolishes KS binding, and the RF in the Fab CH2 domain to prevent Pro-A binding of the hole:hole homodimer. Only the properly paired molecule containing a copy of each light chain would be expected to bind both columns. The Pro-A eluate contained both 2× CODV LC tsAb and 2× Fab LC tsAb in addition to the intact tsCODV. The 2× CODV LC tsAb flowed through the KS column, enabling its removal from the mixture. The neutralized KS eluate was then subjected to Pro-L purification. The Pro-L flow through removed the 2× Fab LC tsAb, resulting in the isolation of the highly purified, properly paired tsCODV in the Pro-L eluate (Figure 11a).

We then tested a second tsCODV tsAb that contained the Pro-L knockout mutation S12P/R18P on the CODV light chain, KS knockout mutation Q199K on the Fab light chain (Vκ2), and RF in the Fab CH2 domain. The same general affinity purification scheme using Pro-A, KS, and Pro-L was applied, but, to test versatility, the order of ProL and KS was reversed. As expected, the 2× Fab LC tsAb was removed in the KS flowthrough, and the 2× CODV LC tsAb was removed in the Pro-L flowthrough (Figure 11b). A half-CODV molecule was also present in the Pro-A eluate for this protein, which was removed by Pro-L purification as expected. These results showed that a method combining the sequential application of KS and Pro-L affinity purification

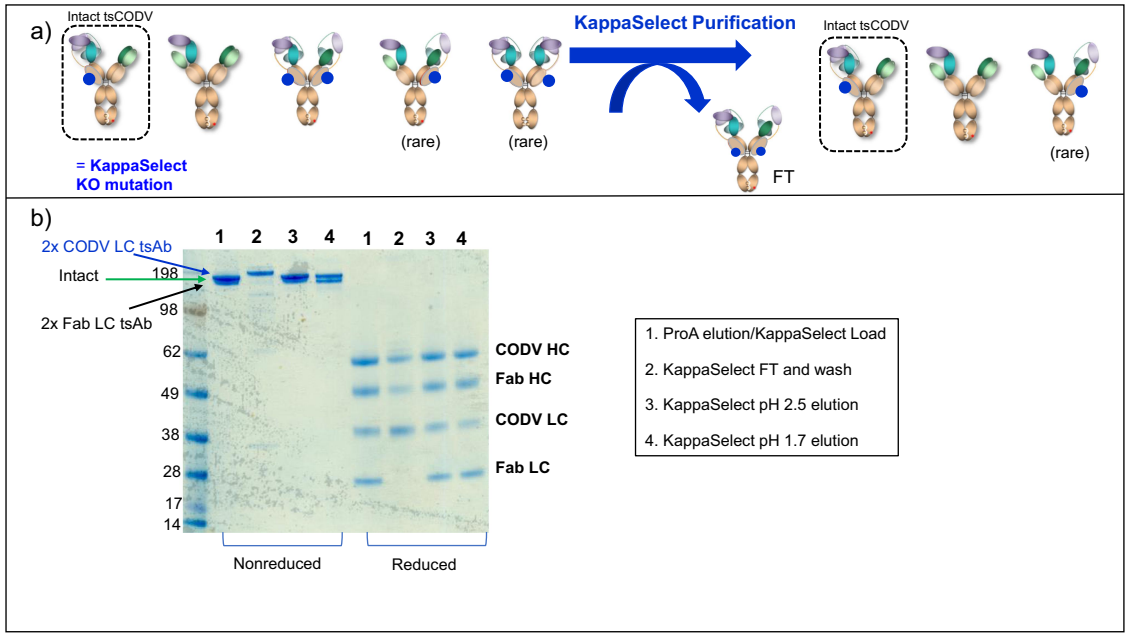

Figure 9. Purification of tsCODV molecules with KS knockout mutation on CODV LC. a. KS purification scheme and expected contents of flowthrough vs. eluate. b. SDS-PAGE comparison of pro-A eluate, KS flow-through, and KS neutralized eluates. In the flow through, only 2× CODV LC tsCODV mis-paired species was detected; while in the KS elution, the correctly paired molecule together with 2× Fab LC tsCODV was detected.

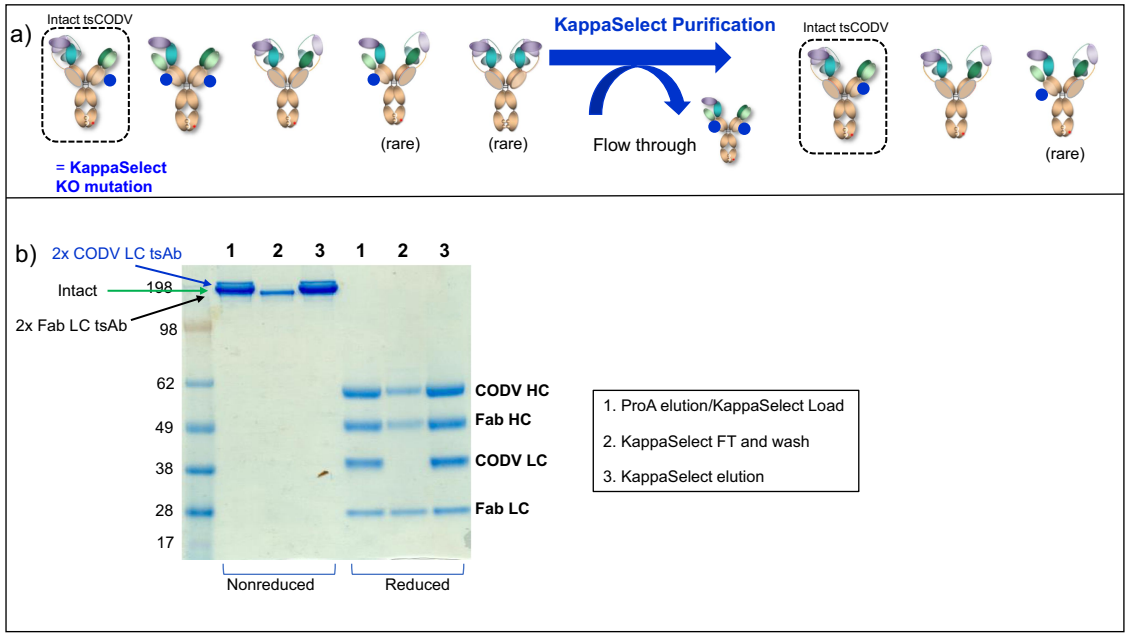

Figure 10. Purification of tsCODV molecules with KS knockout mutation on Fab LC. a. KS purification scheme and expected contents of flowthrough vs. eluate. b. SDS-PAGE comparison of pro-A eluate, KS flow-through, and KS neutralized eluates. In the flow through, only 2× Fab LC tsCODV mis-paired species was detected; while in the KS elution, the correctly paired molecule together with 2× Fab LC tsCODV was detected.

after protein-A purification successfully removes light chain mis-paired species in CODV tsAb.

Removal of multiple mis-paired light chain species in Y-shaped bispecific antibodies using both Pro-L and KS affinity purification

We further tested whether this all affinity-based purification scheme using Pro-A, followed by KS and Pro-L, can be used to remove light chain mis-paired species in Y-shaped IgG-like bispecific antibodies. As a proof-of-concept study, a Y-shaped bispecific antibody consisting of trastuzumab and pertuzumab was constructed using knob-into-hole mutations to eliminate heavy chain homodimerization. The Pro-A eluate of the wild-type protein consisted of mispaired bsAb with 2× trastuzumab light chains, mispaired bsAb with 2× pertuzumab light chains, and the properly paired bispecific antibody as demonstrated by liquid chromatography-mass spectrometry (LC-MS) (Supplemental Figure S4) and analytical hydrophobic interaction chromatography (aHIC) (Figure 12a). To remove light-

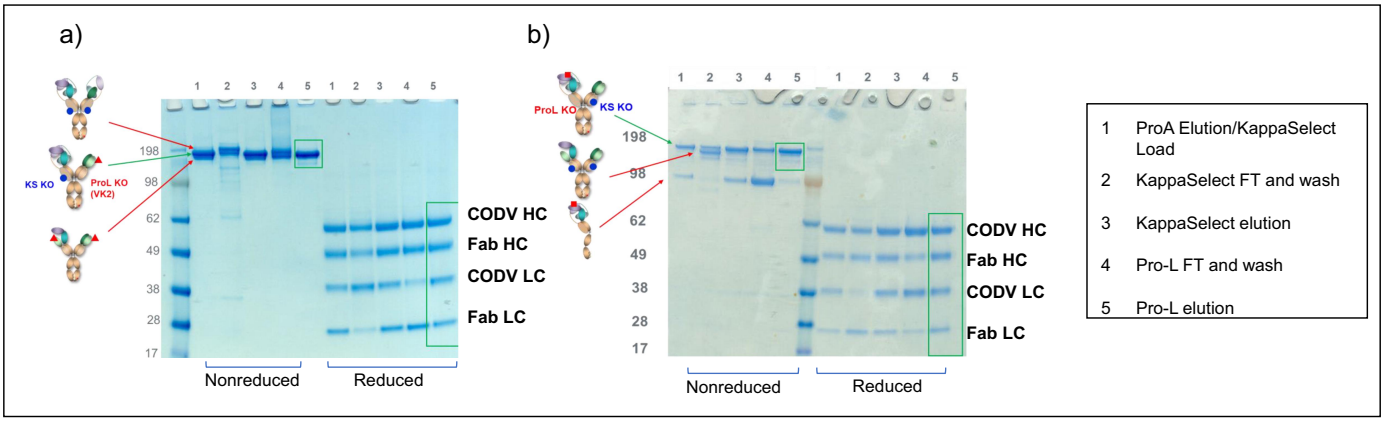

Figure 11. Removal of multiple mis-paired light chain species in two tsCODV's by pro-a, KS, and pro-L purification. a. Fab LC: non-pro-L binding human IgG light chain (Vk2), CODV LC: KS knockout mutation (Q199K). KS flow through contains 2× CODV LC tsAb, pro-L flowthrough contains 2× Fab LC tsAb, and pro-L elution contains correctly paired molecule. b. Fab LC: KS knockout mutation (Q199K), CODV LC: pro-L KO mutation (S12P/R18P). KS flow through contains 2× Fab LC tsAb, pro-L flow through contains CODV LC tsAb (half molecule), and pro-L elution contains correctly paired molecule.

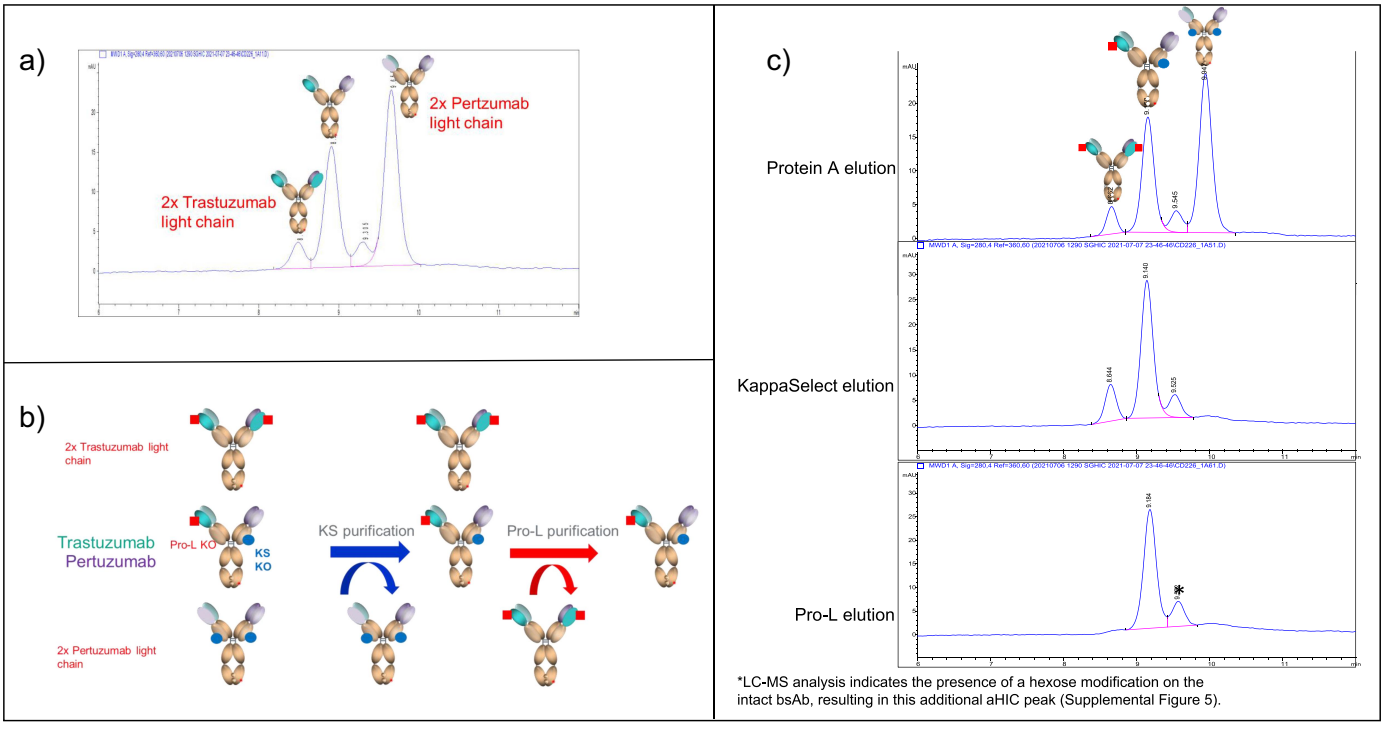

Figure 12. a. aHIC chromatogram of intact and light chain-mispaired species in Y-shape bispecific antibody after pro-A purification. b. Purification scheme for removal of light chain-mispaired species in a Y-shape bispecific antibody using pro-L knockout (S12P/R18P) and KS knockout (Q199K) mutations. c. aHIC chromatogram of intact and light chain-mispaired species after each purification step.

chain mispaired molecules, the Pro-L knockout mutation (S12P/R18P) was introduced into the trastuzumab light chain and the KS knockout mutation (Q199K) was introduced into the pertuzumab light chain. The Pro-A eluate was loaded onto a KS column, which removed the 2× pertuzumab LC species as shown by the disappearance of the indicated aHIC peak in the KS eluate. The neutralized KS eluate was loaded onto a Pro-L column, which removed the 2× trastuzumab LC, as shown by the disappearance of the indicated aHIC peak in the Pro-L eluate (Figure 12c). Unlike tsCODVs, which have significant mass differences between each polypeptide chain, the bsAb chains have similar masses which do not resolve by SDS-PAGE; thus, LC-MS was necessary to confirm the molecule ID of the final purification product. LC-MS analysis also revealed that the protein contains a hexose modification, which corresponds to a second minor peak in the HIC chromatogram for the Pro-L eluate (Figure 12c and Supplemental Figure S4). These results showed that, in addition to tsCODVs, the sequential Pro-A, KS, and Pro-L affinity purification method can efficiently remove light chain-mispaired impurities in Y-shaped bispecific antibodies.

A new affinity purification method consisting of Pro-A, Pro-L and KS affinity purification for bi- and multi-specific antibody

The above data support the potential broad applicability of an all affinity-based purification method in conjunction with the light chain binding knockout mutations across a variety of msAbs (Figure 13). Mutation of amino acids in the CH3 domain ("knobs-into-holes") can be used to favor heterodimerization of the heavy chains, and the inclusion of the "RF" mutation[9] can be used to eliminate "hole-hole" homodimer during the Pro-A purification by eliminating Pro-A binding. In the case of the CODV tsAb molecules, the 2× Fab LC tsAb impurity can be removed using Pro-L affinity by incorporating a Fab light chain mutation to knock out Pro-L binding or by exploiting the presence of a Vκ2 light chain in that position. The 2× CODV LC tsAb impurity can then be removed using KS affinity by incorporating a CODV light chain mutation that knocks out KS binding. The KS and Pro-L knockout mutations can each be positioned on either the Fab or CODV arm, and the order of the KS and Pro-L purification steps can be switched as well. The successful removal of light-chain mispaired species from a Y-shaped bispecific antibody which incorporates these mutations suggests broad applicability to other IgG-based multispecific antibodies.

Discussion

We report here purification-enabling mutations (PEMs) that abolish binding to KS or Pro-L resins to enable an all-affinity-based purification approach for msAbs. These Pro-L and KS binding knockout mutations facilitate removal of light chain mis-paired proteins in both Y-shaped bispecific antibodies and tri-specific CODV formats and have little to no impact on target binding affinity, purity by SEC or SDS-PAGE, thermal stability by nano-DSF, or accelerated stability. Immunogenicity of the mutant adalimumab variants was predicted using a version of netMHC2pan, which considers peptide-MHC binding affinity, eluted ligand immunopeptidomic data, and MHC allele frequencies.[19] The predicted scores for adalimumab containing Pro-L or KS KO mutations are within the range of marketed antibodies (Supplemental Figure S7). In addition to the msAbs reported here, these binding knockout mutations have been successfully applied in other tsCODV discovery campaigns, and we anticipate their use could be extended to other formats beyond those tested here.

The sequences and desired characteristics for lead candidates can evolve significantly during antibody discovery and development. Since the effect of the PEMs on late-stage development properties such as manufacturability and deviceability remains to be explored, we recommend application of the PEM technology during early-stage screening and scale-up. One important step in our msAb discovery workflow is the selection of lead candidates that are produced on a high-throughput protein expression and purification platform. At this stage, 100–500+ msAbs are expressed at small scale and purified by a single affinity step. As a result, they typically contain significant amounts of product-related impurities that can interfere with the assays and analytics used for lead selection. Introduction of the PEMs at this stage would enable high-throughput removal of product-related impurities so that lead selection would be based on pure rather than mixed material.

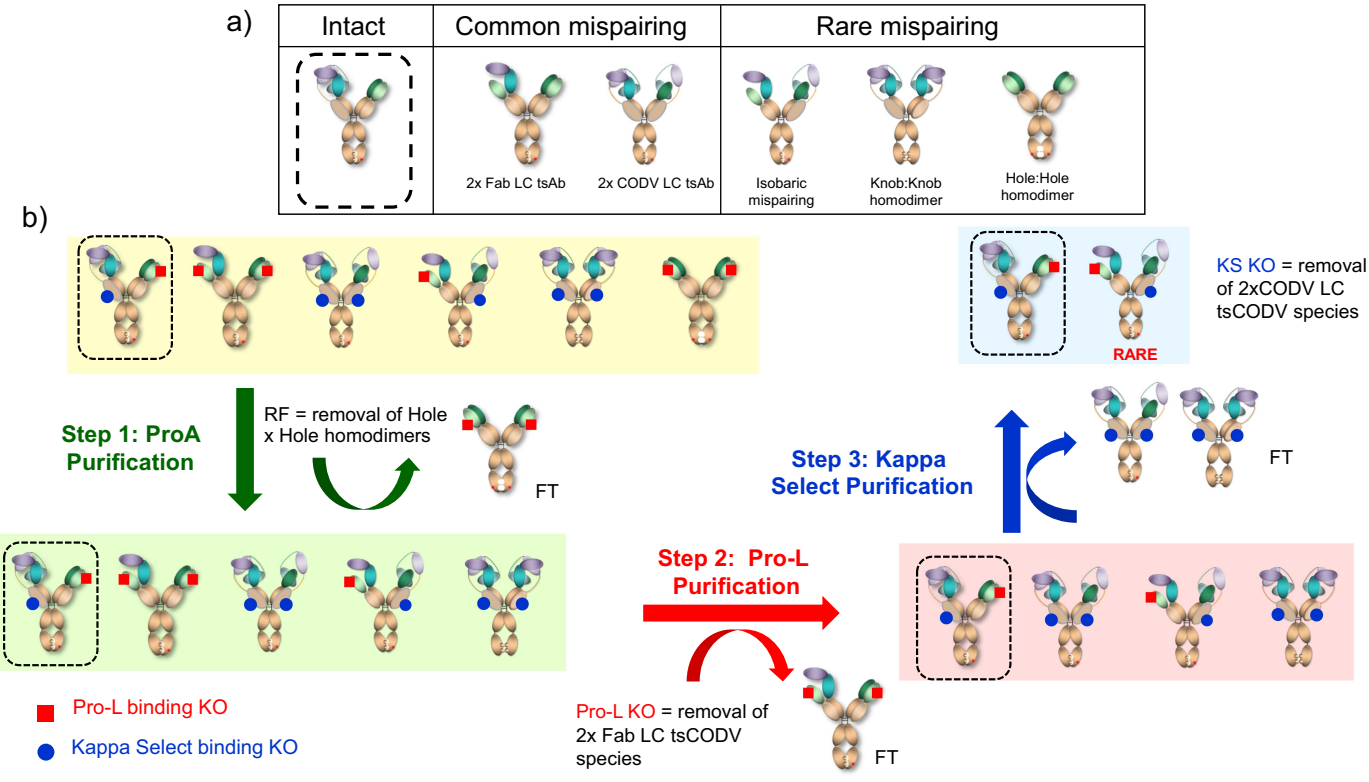

Figure 13. a. Intact and chain-mispaired trispecific CODV antibodies (tsCODV). b. Envisioned all-affinity purification scheme for removing chain-mispaired tsCODVs by introducing mutations that ablate pro-L or KS binding.

The introduction of PEMs would also facilitate scale-up (~10–200 mg) production of lead candidates. Typically, these msAbs are purified using Pro-A, followed by IEX and SEC purification, which results in significant yield reduction due to incomplete separation of the protein of interest from mispaired species. Using an all affinity-based purification scheme could enable more complete separation and thus higher recovery of the protein of interest. Affinity-based purification methods can be done in parallel on most setups and do not require buffer exchange between steps, which makes the process much more rapid than gradient-based ion-exchange methods.

Multi-specific antibodies have the potential to make a significant impact in many therapeutic areas that have been recalcitrant to modulation by monospecific antibodies. Overcoming the production challenges associated with separating the correctly paired molecule from chain-mispaired proteins will accelerate the discovery and development of lead molecules. Application of the PEM technology presented here facilitates purification of virtually any IgG-like multispecific antibodies that may undergo light chain mispairing during early-stage screening and scale up of therapeutic candidates.

Materials and methods

Cell culture

Expi293F cells were maintained in shake flasks under standard culture conditions. Cells were seeded to 2.8×10^6 vc/mL on the day of transfection and then transfected using the Expifectamine293 kit (Thermo Fisher: A14525) according to the manufacturer's instructions. Feeds were added 24 h after transfection. Cell culture was harvested after 4–7 days of expression and clarified using a diatomaceous earth-based clarification kit (Sartorious: SDLV-1000-10E0-2). Cell culture supernatant was filtered using a 0.2 um PES filter unit to remove any particulates prior to loading onto the column.

Pro-A affinity purification

Column: mAbSelect SuRe (Cytiva #11-0034-95), Dimensions: 5 mL column (16 mm x 25 mm), Default flow rate: 5 mL/min (max ~20 mL/min).

Column was sanitized with 4 column volumes (CV) of Buffer A (0.2 M NaOH), rinsed with 5 CV MilliQ water, and equilibrated with 15 CV Buffer B (20 mm sodium phosphate, 150 mm NaCl, pH 7.2). Cell culture supernatant was loaded onto the column and washed with 10 CV Buffer B. Antibody was eluted with 5 CV Buffer C (50 mm sodium acetate, pH 3.5) into a tube containing 1/10 volume (2.5 mL) 1 M Tris pH 10.2 to neutralize. No buffer exchange was performed prior to the second affinity purification step.

KS affinity purification

Column: HiTrap KS 5×1 mL (Cytiva #17545811), Dimensions: 1 mL pre-packed column, Default flow rate: 1 mL/min. Sample input: neutralized Pro-A eluate from mAbSelect SuRe purification. Load volume was calculated to stay within the binding capacity of KappSelect resin (15 mg IgG/mL resin).

Column was sanitized with 10 CV Buffer D (10 mm NaOH, pH 12) for 15-min contact time, rinsed with 5 CV MilliQ water, and equilibrated with 10 CV Buffer B. Neutralized Pro-A eluate from mAbSelect SuRe purification was loaded onto KS column(s) and washed with 10 CV Buffer B. Protein was eluted with 5 CV 100 mm Glycine-HCl, pH 2.4 in a tube containing 1/10 volume 1 M Tris pH 10.2 to neutralize to pH 7–8.

Pro-L affinity purification

Column: Thermo Scientific 89,929 Pierce Chromatography Cartridges Pro-L, 1×5 mL. Dimensions: 1 mL prepack column, default flow rate: 1 mL/min. Sample input: neutralized protein eluate from KS purification. Load volume was calculated to stay within the binding capacity of Pro-L resin (4–5 mg human IgG/mL of resin).

Column was sanitized with 10 CV Buffer D for 15-min contact time, rinsed with 5 CV MilliQ water, and equilibrated with 10 CV Buffer B. Neutralized protein eluate from KS purification was loaded onto Pro-L column(s) and washed with 10 CV Buffer B. Protein was eluted with 5 CV 100 mm Glycine-HCl, pH 2.4 into a tube containing 1/10 volume 1 M Tris pH 10.2 to neutralize to pH 7–8.

SDS-PAGE

Five micrograms of each protein sample were prepared with LDS loading dye (Life Technologies: NP0007) plus NuPAGE reducing buffer for reduced samples (Life Technologies: NP009). Samples were loaded onto a 4–12% NuPAGE Bis-Tris mini gel (Life Technologies: NP0321BOX) and run according to the manufacturer's instructions using 1X MES running buffer. Gel was stained with Instant Blue Coomassie stain (AbCam: ab119211).

Analytical size-exclusion chromatography

Five micrograms of each protein were analyzed on a TSKgel SuperSW3000 column (Tosoh Bioscience: 18675) using a 40 mm sodium phosphate buffer with 200 mm arginine, pH 7.0 mobile phase on an Agilent 1260 hPLC system equipped with A280 detection.

Analytical hydrophobic interaction chromatography

Twenty micrograms of each protein were analyzed on a MabPac HIC-10 column (5 μm, 4.6×250 mm, Thermo Fisher Cat No 088481). Running buffer A: 1.5 M ammonium sulfate, 25 mm sodium phosphate pH 7.0. Buffer B: 25 mm sodium phosphate pH 7.0. The protein was injected onto the column and separated using a linear gradient from 30% to 100% column B over 11 min at a flow rate of 0.6 mL/min.

Biolayer interferometry (Octet)

Adalimumab wild-type, Pro-L knockout mutants, and a lambda light chain negative control antibody were diluted to 100 nM in binding buffer (phosphate-buffered saline (PBS), pH 7.4, with 1 mg/mL bovine serum albumin), then loaded onto anti-human IgG Fc Capture biosensor (Sartorius, 18–5060) to a density of 1.0 nm using a BLI system (Octet RED96e, ForteBio). After equilibrium, binding to 100 nM recombinant Pro-L (Pierce™ 2118) was performed using 180-s of association and 180-s of dissociation at 25°C. Binding responses were captured, and binding affinity was fitted using a 1:1 binding model.

NanoDSF characterization

Adalimumab with or without a Pro-L knockout mutation was buffered exchanged into 10 mm pH 6.0 histidine buffer and concentration-normalized to 0.5 mg/mL. Nine microliters of the sample were loaded into the respective capillaries (NanoTemper PR-C006 on a NanoTemper Prometheus instrument), and the temperature was equilibrated at 20°C for 3 min before ramping up to 95°C at 1°C/min. The fluorescence emission (330 nm and 350 nm) was recorded as a function of temperature. The maxima of the first derivative of the ratio of fluorescence intensities at 330 nm and 350 nm as a function of temperature were used to determine the melting temperatures of the proteins.

Differential scanning calorimetry

One milligram of adalimumab, with or without KS knockout mutations, was digested with IdeZ protease (New England Biolabs, P0770S) at 37°C overnight. The next day, 5 μg of digested protein was analyzed on SDS-PAGE to confirm the complete cleavage of F(ab)'2 from Fc. The remaining protease-digested antibody samples were loaded on 1 mL of CaptureSelect CH1-XL affinity resin (Thermo Scientific 494,346,201). After washing with PBS, the samples were eluted with 5 CV of 0.1 M glycine buffer pH 2.5, and neutralized with 1 M Tris pH 9.0. Samples were buffer exchanged into 10 mm histidine pH 6.0, and DSC was performed on a MicroCal PEAQ-DSC system (Malvern Panalytical) from 15°C to 105°C, at 200°C/h scan rate. After background subtraction with a buffer-only reference, the protein's heat capacity (Cp) as a function of temperature was shown. T_m (melting point) was calculated from the melting curve.

LC-MS

Three micrograms of each sample was injected onto an Agilent 1290 hPLC instrument equipped with a PLRP-S column (Agilent: PL-1912–1502) operating at a flow rate of 0.3 mL/min. Protein was separated using a linear gradient of water and acetonitrile, each with 0.1% formic acid, and injected into the Agilent 6545XT Q-TOF. Source conditions are as follows: gas temp 350°C, drying gas 12 L/min, nebulizer pressure 60 psi, sheath gas temp 400°C, sheath gas flow 11 L/min, Vcap 5500 V, nozzle voltage 2000 V, fragmentor voltage 380 V, and skimmer voltage 140 V. Data was deconvoluted and analyzed using Protein Metrics Byos software.

Acknowledgments

We would like to thank Dietmar Hoffmann, May Cindhuchao, Shyanne Temple, Karen Wong, and Jennifer Buell for DNA design and preparation. We would like to thank Sagar Kathuria for assistance with the DSC and DSF experiment setup.

Disclosure statement

K. Mix, B. Hall, J. Newton, C. Eng, Y. Guo, and D. Reczek are employees of Sanofi and may hold stocks or shares in the company.

Funding

The author(s) reported there is no funding associated with the work featured in this article.

ORCID

Kalie Mix http://orcid.org/0000-0002-2836-5744

References

1. Mullard A. FDA approves 100th monoclonal antibody product. Nat Rev Drug Discov. 2021;20(7):491–495. doi: 10.1038/d41573-021-00079-7.
2. Kaplon H, Chenoweth A, Crescioli S, Reichert JM. Antibodies to watch in 2022. MAbs. 2022;14(1):14. doi: 10.1080/19420862.2021.2014296.
3. Haslam A, Prasad V. Estimation of the percentage of US patients with cancer who are eligible for and respond to checkpoint inhibitor immunotherapy drugs. JAMA Netw Open. 2019;2(5):e192535–e192535. doi: 10.1001/jamanetworkopen.2019.2535.
4. Wood L. Global bispecific antibody market to 2028- opportunity, drug sales, price & clinical trials insights -Research And Markets.com. Dublin, Ireland: Business Wire; 2021 [accessed June 28].
5. Nie S, Wang Z, Moscoso-Castro M, D'Souza P, Lei C, Xu J, Gu J. Biology drives the discovery of bispecific antibodies as innovative therapeutics. Antibody Ther. 2020;3(1):18–62. doi: 10.1093/abt/tbaa003.
6. Labrijn AF, Janmaat ML, Reichert JM, Parren P. Bispecific antibodies: a mechanistic review of the pipeline. Nat Rev Drug Discov. 2019;18(8):585–608. doi: 10.1038/s41573-019-0028-1.
7. Steinmetz A, Vallée F, Beil C, Lange C, Baurin N, Beninga J, Capdevila C, Corvey C, Dupuy A, Ferrari P, et al. CODV-Ig, a universal bispecific tetravalent and multifunctional immunoglobulin format for medical applications. mAbs. 2016;8(5):867–878. doi: 10.1080/19420862.2016.1162932.
8. Ridgway JBB, Presta LG, Carter P. 'Knobs-into-holes' engineering of antibody CH3 domains for heavy chain heterodimerization. Protein Eng Des Sel. 1996;9(7):617–621. doi: 10.1093/protein/9.7.617.
9. Tustian AD, Endicott C, Adams B, Mattila J, Bak H. Development of purification processes for fully human bispecific antibodies based upon modification of protein a binding avidity. MAbs. 2016;8(4):828–838. doi: 10.1080/19420862.2016.1160192.
10. Krah S, Kolmar H, Becker S, Zielonka S. Engineering IgG-like bispecific antibodies—an overview. Antibodies. 2018;7(3):28. doi: 10.3390/antib7030028.
11. Schaefer W, Regula JT, Bähner M, Schanzer J, Croasdale R, Dürr H, Gassner C, Georges G, Kettenberger H, Imhof-Jung S, et al. Immunoglobulin domain crossover as a generic approach for the production of bispecific IgG antibodies. Proc Natl Acad Sci USA. 2011;108(27):11187–11192. doi: 10.1073/pnas.1019002108.

12. Bönisch M, Sellmann C, Maresch D, Halbig C, Becker S, Toleikis L, Hock B, Rüker F. Novel CH1: CL interfaces that enhance correct light chain pairing in heterodimeric bispecific antibodies. Protein Eng, Des Selection. 2017;30(9):685–696. doi: 10.1093/protein/gzx044.
13. Wu X, Sereno AJ, Huang F, Zhang K, Batt M, Fitchett JR, He D, Rick HL, Conner EM, Demarest SJ. Protein design of IgG/TCR chimeras for the co-expression of fab-like moieties within bispecific antibodies. mAbs. 2015;7(2):364–376. doi: 10.1080/19420862.2015.1007826.
14. Nesspor TC, Kinealy K, Mazzanti N, Diem MD, Boye K, Hoffman H, Springer C, Sprenkle J, Powers G, Jiang H, et al. High-throughput generation of bipod (fab × scFv) bispecific antibodies exploits differential chain expression and affinity capture. Sci Rep. 2020;10(1):7557. doi: 10.1038/s41598-020-64536-w.
15. Ereño-Orbea J, Sicard T, Cui H, Carson J, Hermans P, Julien J-P. Structural basis of enhanced crystallizability induced by a molecular chaperone for antibody antigen-binding fragments. J Mol Biol. 2018;430(3):322–336. doi: 10.1016/j.jmb.2017.12.010.
16. Nilson BHK, Lögdberg L, Kastern W, Björck L, Åkerström B. Purification of antibodies using protein L-binding framework structures in the light chain variable domain. J Immunol Methods. 1993;164(1):33–40. doi: 10.1016/0022-1759(93)90273-A.
17. Chen C, Wakabayashi T, Muraoka M, Shu F, Wei Shan C, Chor Kun C, Tim Jang C, Soehano I, Shimizu Y, Igawa T, et al. Controlled conductivity at low pH in protein L chromatography enables separation of bispecific and other antibody formats by their binding valency. mAbs. 2019;11(4):632–638. doi: 10.1080/19420862.2019.1583996.
18. Graille M, Harrison S, Crump MP, Findlow SC, Housden NG, Muller BH, Battail-Poirot N, Sibaï G, Sutton BJ, Taussig MJ, et al. Evidence for plasticity and structural mimicry at the immunoglobulin light chain-protein L interface. J Biol Chem. 2002;277(49):47500–47506. doi: 10.1074/jbc.M206105200.
19. Birkir Reynisson CB, Barra C, Kaabinejadian S, Hildebrand WH, Peters B, Nielsen M. Improved prediction of MHC II antigen presentation through integration and motif deconvolution of mass spectrometry MHC eluted ligand data. J Proteome Res. 2020;19(6):2304–2315. doi: 10.1021/acs.jproteome.9b00874.